



Journal of Advanced Research in Fluid Mechanics and Thermal Sciences

Journal homepage:
https://semarakilmu.com.my/journals/index.php/fluid_mechanics_thermal_sciences/index
ISSN: 2289-7879



Effects of Arrhenius Activation Energy on Thermally Radiant Williamson Nanofluid Flow Over a Permeable Stretching Sheet with Viscous Dissipation

Swarna Jannapura Bhaskar Acharya¹, Bommanna Lavanya^{1,*}, Kolli Vijaya², Manikandan Murugiah³

¹ Department of Mathematics, Manipal Institute of Technology, Manipal Academy of Higher Education, Manipal, Karnataka-576104, India

² Department of Mathematics, Geethanjali Institute of Science and Technology, Gangavaram, Nellore AP 524137, India

³ Department of Aeronautical & Automobile Engineering, Manipal Institute of Technology, Manipal Academy of Higher Education, Manipal, Karnataka-576104, India

ARTICLE INFO

Article history:

Received 24 January 2024

Received in revised form 27 May 2024

Accepted 15 June 2024

Available online 30 June 2024

Keywords:

Williamson nanofluid; stretching sheet; viscous dissipation; electrically conducting fluid; thermal radiation; Arrhenius activation energy

ABSTRACT

This paper explores the role of viscous dissipation, Arrhenius activation energy, and thermal radiation of Williamson nanofluid flow over a permeable stretching sheet. The governing partial differential equations have been simplified through a transformation process, resulting in a set of non-linear differential equations. To find a solution for these equations, a numerical approach is employed, specifically the fourth order Runge-Kutta method. Additionally, a shooting technique is utilized to enhance the accuracy of the numerical solutions. Overall, the study involves reducing complex equations, solving them numerically, and refining the results through a combination of methods. The study investigates the impact of different physical parameters on key factors like velocity, temperature, skin friction coefficient, nano particle volume fraction, and rates of mass and heat transfer. This study exhibits that activation energy parameter enhances concentration profiles, whereas fitted rate constant shows opposite behavior. The activation energy into heat transfer model allows for the optimization of heat transfer systems utilizing Williamson nano fluids.

1. Introduction

Nanofluids, suspensions of nanoparticles in fluids, demonstrate improved heat transfer in heat exchangers, making them valuable in various applications. Nanofluids has unique thermal conductivity due to that they are widely used in various fields. Nanoparticles find applications in diverse fields such as cell separation, drug delivery, magnetic resonance imaging, heat dissipation, damping, and dynamic ceiling. Their improved thermal and rheological properties make nanofluids effective in enhancing heat exchanger performance. Additionally, the study of convective fluid flow on porous mediums is crucial in numerous science and engineering systems, including nuclear waste disposal, heat exchanger layouts, groundwater systems, crude oil production, and more. Researchers

* Corresponding author.

E-mail address: lavanya.b@manipal.edu

<https://doi.org/10.37934/arfmts.118.2.181195>

focus on studying chemical reactions and activation energy for industrial applications such as fibrous insulation, fog formation, cooling of nuclear reactors, thermal oil recovery, etc.

Yang *et al.*, [1] explored nanofluid thermal performance with and without a magnetic field, concluding with theoretical models for thermal conductivity and viscosity. Ali and Salam [2] highlighted diverse nanofluid applications, including heat exchangers, transportation, cooling, refrigeration, transformer oil, desalination, and nuclear systems, emphasizing recent developments in heat transfer enhancement using nanofluids. using Homotopy perturbation technique Saxena's [3] research focused on studying the impact of viscous dissipation and heat transfer convection across flat plate. Li *et al.*, [4] reviews about the thermal conductivity of a nanofluid. Many new nanofluids are prepared such as cellulose nanofluid, graphene nanofluids, etc. Adnan *et al.*, [5] inferred that ND-H₂O and Ag-H₂O has high thermal performance characteristics. They have observed that Ag based nanofluid has higher heat transfer performance. Ajibade *et al.*, [6] explored the influences of magnetic field, suction/injection, porous material permeability, and viscous dissipation on an electrically conducting incompressible fluid in a vertical porous channel. Rehman *et al.*, [7] analysed the fluctuating motion of nanofluid film across flexible surface. using Casson fluid over an upper horizontal melt surface. Ajayi *et al.*, [8] studied the effects of viscous dissipation. This paper is analysis on boundary layer. Hassan *et al.*, [9] explored the impact of heat radiation on 2D magneto hydrodynamic Casson fluid flow, considering viscous dissipation, chemical reaction, and heat generation/absorption. Eswaramoorthi *et al.*, [10] investigated MHD flow of Williamson nanofluid over a deformable plate, emphasizing the influence of heat radiation. Khan and Pop studied nanofluid behaviour over a stretching sheet. Khan and Pop [11] studied the characteristics of nanofluid across flexible sheet. Pearson and Tardy [12] have explained how non-Newtonian and complex fluids are behaved when they passed through a porous medium. Kalaivanan *et al.*, [13] reviewed the Arrhenius activation energy of a second grade nanofluid. Mozafarie and Javaherdeh [14] investigated the transfer of non-Newtonian solution through a double- pipe heat exchanger with coiled fins encompassing the inner tube. Their findings highlighted the induction of swirling flow patterns in the annulus by the helical fin. In their study, Sheikholeslami *et al.*, [15] investigated the impact of a non-uniform magnetic field on forced convection heat transfer in Fe₃O₄-H₂O nanofluid. The analysis focused on the influence of Reynolds number, nanoparticle volume fraction, and Hartmann number on the flow and heat transfer properties of the nanofluid. Li *et al.*, [16] discussed the advancements in nanofluid studies, covering preparation methods, stability mechanisms, and strategies for enhancing fluid stability. They highlighted potential implementation in heat transfer, mass transfer, energy, mechanics, and biomedicine. Rasheed *et al.*, [17] explored nanofluid behaviour on an elongated moving surface under a uniform hydromagnetic field and heat reservoir. Using Rossland diffusion approximation and Stephan's law with MHD effects, they formulated constitutive flows. Gireesha and Rudraswamy [18] have addressed nanofluid behaviour near the stagnation point on a permeable stretching surface. Their model considered Brownian motion, thermophoresis, a uniform magnetic field, and non-uniform heat source/sink, including the influence of chemical reactions. Sheri and Thumma [19] provided a numerical solution for magnetohydrodynamic free convection flow of a nano liquid along a vertical plane, incorporating porous medium and radiation effects. Choi and Eastman [20] suggested creating a novel category of heat transfer fluids by incorporating metallic nanoparticles into traditional heat transfer fluids. Nadeem and Hussain [21], Krishnamurthy *et al.*, [22], Gorfie *et al.*, [23], and Lavanya [24] studied about MHD fluids.

The Arrhenius activation energy is defined as the minimum amount of energy required for a chemical reaction to occur. It represents the energy difference between the reactants and the transition state or activated complex. The concept of Arrhenius activation energy has numerous practical applications across various fields of science and technology. Activation energy help us to

predict and control the rate of chemical reaction. It helps in designing reaction conditions to optimize the rate of desired reactions in chemical synthesis and industrial processes. It plays a crucial role in understanding the kinetics of material transformation processes such as phase transitions, diffusion, and nucleation. It helps in predicting the stability, durability, and performance of materials under different conditions. Activation energy is relevant in environmental science for understanding the kinetics of chemical reactions involved in atmospheric chemistry, pollutant degradation, and remediation processes. It helps in understanding the rates of biochemical reactions within living organisms and designing drugs that can selectively inhibit or enhance specific enzymatic reactions based on their activation energies. Overall, the concept of Arrhenius activation energy is fundamental in understanding the temperature dependence of reaction rates and plays a crucial role in various fields such as chemistry, biochemistry, and material science.

Kumar *et al.*, [25] analysed the effect of Arrhenius activation energy in magnetohydrodynamic Carreau fluid flow through improved theory of heat diffusion and binary chemical reaction. Vijaya *et al.*, [26] examined the behaviour of Arrhenius activation energy in electrically conducting Casson fluid flow in induced due to permeable elongated sheet with chemical reaction and viscous dissipation. Nagasakala and Lavanya [27] investigated the heat and mass transfer characteristics of a magnetohydrodynamic (MHD) flow of a nanofluid passing through a porous medium within an annular, circular region, where the outer cylinder is subjected to a constant heat flux. Akaje and Olajuwon [28] studied the impacts of nonlinear radiative heat on the species heat transfer of a MHD Casson nanofluid flow with stagnation point associated with Thompson and Troian boundary conditions. Primitive and gravity modulation of periodical heat transfer along magnetic-driven porous cone with thermal conductivity and surface heat flux studied by Al-Shammari *et al.*, [29]. Ullah *et al.*, [30] studied Oscillatory and Periodical Behaviour of Heat Transfer and Magnetic Flux along Magnetic-Driven Cylinder with Viscous Dissipation and Joule Heating Effects.

This paper explores the role of viscous dissipation, Arrhenius activation energy, and thermal radiation of Williamson nanofluid flow over a permeable stretching sheet. The governing partial differential equations have been simplified through a transformation process, resulting in a set of non-linear differential equations. To find a solution for these equations, a numerical approach is employed, specifically the fourth order Runge-Kutta method. Additionally, a shooting technique is utilized to enhance the accuracy of the numerical solutions. Overall, the study involves reducing complex equations, solving them numerically, and refining the results through a combination of methods. The use of Arrhenius activation energy in Williamson nanofluid research facilitates a deeper understanding of temperature dependent properties and behaviour, which is essential for designing and optimising nanofluid based thermal management system.

2. Methodology

The study investigates the steady two-dimensional flow of a Williamson nanofluid which is incompressible, thermally radiant, electrically conducting over a permeable stretching sheet in a uniform free stream shown in Figure 1. The analysis includes considerations of viscous dissipation and Arrhenius activation energy. The condition involves a stretching parameter, velocity profiles of the free stream, stretching sheet, and the application of a uniform external magnetic field. Because of the existence of an external magnetic field, the nanofluid exhibits less likelihood of electron collisions with other particles. Temperature and concentration values T_w and C_w at the moving surface are assumed to be constant. Under the specified conditions, the governing equations for the boundary layer describe the momentum, energy, and diffusion of a steady two-dimensional flow of a Williamson nanofluid over a permeable stretching sheet in a uniform free stream.

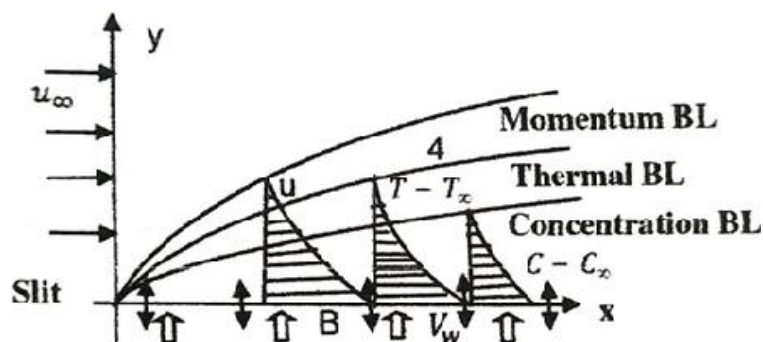


Fig. 1. Schematic representation of the flow

With respect to all the above conditions the equations account for the influence of viscous dissipation and Joule heating on the nanofluid's behaviour within the free stream may be written as,

$$\frac{\partial u}{\partial x} + \frac{\partial v}{\partial y} = 0 \quad (1)$$

$$u \frac{\partial u}{\partial x} + v \frac{\partial u}{\partial y} = \nu \frac{\partial^2 u}{\partial y^2} + \sqrt{2} \nu \Gamma \frac{\partial u}{\partial y} \frac{\partial^2 u}{\partial y^2} + u_\infty \frac{\partial u_\infty}{\partial x} + \frac{\sigma B_0^2}{\rho} (u_\infty - u) \quad (2)$$

$$u \frac{\partial T}{\partial x} + v \frac{\partial T}{\partial y} = \alpha \frac{\partial^2 T}{\partial y^2} + \frac{\nu}{c_p} \left[\left(\frac{\partial u}{\partial y} \right)^2 + \sqrt{2} \Gamma \left(\frac{\partial u}{\partial y} \right)^3 \right] + \tau \left[D_B \frac{\partial C}{\partial y} \frac{\partial T}{\partial y} + \frac{D_T}{T_\infty} \left(\frac{\partial T}{\partial y} \right)^2 \right] + \frac{\sigma B_0^2}{\rho c_p} (u_\infty - u)^2 - \frac{1}{\rho c_p} \frac{\partial q_r}{\partial y} \quad (3)$$

$$u \frac{\partial C}{\partial x} + v \frac{\partial C}{\partial y} = D_B \frac{\partial^2 C}{\partial y^2} + \frac{D_T}{T_\infty} \frac{\partial^2 T}{\partial y^2} - K_r (C - C_\infty) \left(\frac{T}{T_\infty} \right)^n \exp \left(-\frac{E_a}{xT} \right) \quad (4)$$

where u and v represent the velocity components in the x and y direction respectively; T is temperature and C is nanoparticle volume fraction; σ , α and c_p represent electrical conductivity, thermal diffusivity, and specific heat capacity of the nanofluid; D_B , D_T , K_r and Γ represent Brownian diffusion coefficient, thermophoresis diffusion coefficient, chemical reaction constant and time constant; ρ , ν and k denote density, kinematic viscosity and thermal conductivity of the nanofluid; q_r denote radiative heat flux, $\tilde{\tau}$ indicates the ratio of thermal capacities between the fluid and nanoparticles.

In reference to the differential equations, the boundary constraints are:

$$u = U_\infty, \quad v = -V_w, \quad T = T_w, \quad C = C_w, \quad \text{at } y = 0$$

$$u \rightarrow u_\infty, \quad T \rightarrow T_\infty, \quad C \rightarrow C_\infty, \quad \text{as } y \rightarrow \infty \quad (5)$$

where T_∞ and C_∞ are respectively, temperature and nanoparticles volume fraction away from the sheet. The term V_w represents mass suction/ injection velocity. It expresses the mass to be transferred at the surface with $V_w > 0$ for suction and $V_w < 0$ for injection.

The heat radiative flux q_r , via the Rosseland diffusion approximation, is specified as

$$q_r = -\frac{4\sigma^*}{3k^*} \frac{\partial T^4}{\partial y} \quad (6)$$

where k^* is a mean absorption coefficient and σ^* is the Stefan –Boltzmann constant. Given the assumption that as temperature variation in the flow are fairly minor, T^4 represented as a linear function of T

$$T^4 \approx 4T_\infty^3 T - 3T_\infty^4 \quad (7)$$

in (6) and Using (7) then the substitution of its value in Eq. (3), gives

$$\frac{\partial q_r}{\partial y} = -\frac{16\sigma^* T_\infty^3}{3k^*} \frac{\partial^2 T}{\partial y^2} \quad (8)$$

To reduce governing formulas to an ode system, the transformation equations listed below are established.

$$\eta = y \sqrt{\frac{a}{\nu}},$$

$$T = T_\infty + (T_w - T_\infty)\theta(\eta), \quad (9)$$

$$C = C_\infty + (C_w - C_\infty)\varphi(\eta),$$

$$\Psi = \sqrt{avx}f(\eta),$$

where θ represents temperature, stream function denoted as f , ω is nanoparticles volume fraction and η is a similarity variable. Here θ , f and ω are dimensionless component. The velocity components are specified as $u = \partial \psi / \partial y$ and $v = -\partial \psi / \partial x$, which identically meets the continuity Eq. (1). The stream function ψ is introduced. Using the governing equations' similarity variables (2) to (4) give

$$f''' + ff'' + Wef''f''' - f'^2 + M(A - f') + A^2 = 0 \quad (10)$$

$$\left(1 + \frac{4}{3} Rd\right)\theta'' + Pr(f\theta' + Ec(f''^2 + Wef''^3 + Mf'^2) + Nb\theta'\varphi' + Nt\theta'^2) = 0 \quad (11)$$

$$\varphi'' + Scf\varphi' + \frac{W_t}{W_b}\theta'' - Sc\sigma\varphi[1 + \delta\theta]^n \exp\left(-\frac{z}{1+\delta\theta}\right) = 0 \quad (12)$$

and the associated boundary constraints become:

$$f(0) = S, \quad f'(0) = 1, \quad \theta(0) = 1, \quad \varphi(0) = 1$$

$$f'(\eta) \rightarrow A, \quad \theta(\eta) \rightarrow 0, \quad \varphi(\eta) \rightarrow 0, \quad \text{as } \eta \rightarrow \infty \quad (13)$$

Here, primes denote differentiation with respect to η .

The local Nusselt number Nu_x , local Sherwood number Sh_x and skin-friction coefficient C_f are the values we are interested in studying wall heat and mass transfer rate, and surface drag are all described by these numbers, in the order. The definition of the quantities is

$$C_f = \frac{\tau_w}{\rho U_w^2}, \quad Nu_x = \frac{xq_w}{k(T_w - T_\infty)}, \quad Sh_x = \frac{xJ_w}{D_B(C_w - C_\infty)} \quad (14)$$

where the mass and heat flux, temperature difference and shear stress at the surface are denoted by J_w , q_w , δ and τ_w respectively and are defined as

$$\tau_w = \mu \left[\frac{\partial u}{\partial y} + \frac{\Gamma}{\sqrt{2}} \left(\frac{\partial u}{\partial y} \right)^2 \right]_{y=0}$$

$$q_w = - \left(k + \frac{16\sigma^* T_\infty^3}{3k^*} \right) \left(\frac{\partial T}{\partial y} \right)_{y=0} \quad (15)$$

$$J_w = -D_B \left(\frac{\partial C}{\partial y} \right)_{y=0}$$

$$\delta = \frac{T_w - T_\infty}{T_\infty}$$

By applying Eq. (14) and Eq. (15), the wall mass and heat transfer rates, skin friction coefficient (surface drag), are as follows:

$$Nu_x = - \left(1 + \frac{4}{3} Rd \right) \sqrt{Re_x} \theta'(0) , \quad Sh_x = -\sqrt{Re_x} \phi'(0)$$

and

$$\sqrt{Re_x} C_f = f''(0) + \frac{We}{2} f''^2(0) \quad (16)$$

where the local Reynolds number represented as $Re_x = xU_w/\nu$.

3. Numerical Solution

Eq. (10) to Eq. (12) are highly nonlinear, making it challenging, and perhaps even impossible, to obtain closed-form solutions. Consequently, the approach taken to solve these boundary value problems involves numerical methods. Specifically, a conventional fourth-order Runge-Kutta (RK) integration scheme is employed in conjunction with the shooting technique to numerically solve the problems. This combination of numerical techniques helps approximate solutions for the complex nonlinear equations.

To initiate the computation, the first step involves transforming the boundary value problem into an initial value problem.

Let $f = y(1)$, $f^1 = y(2)$, $f'' = y(3)$, $f''' = y(4)$, γ -variance = $y(5)$, γ -prime = $y(6)$, $z = y(7)$, z -prime = $y(8)$, $y' = f'$, $y'' = f''$, $y''' = f'''$.

$$y^{IV} = -f * f'' - f * f''' + w * f'' * f''' - (f')^2 + M * (A - f') + A^2 \quad (17)$$

$$y^V = y'$$

$$y^{IV} = -Pr * f * y' + Ec(f'')^2 + w(f'')^3 + M(f')^2 + Wby'z' + Nt(y')^2/(1 + 4/3)Rd \quad (18)$$

$$y^7 = z'$$

$$y^8 = -Sc * f * z' - (Wt/Wb)f'' - Sc * \sigma * \varphi(1 + \delta\theta)^n \exp(-E/1 + \delta\theta) \quad (19)$$

With the boundary conditions

$$S=1, y' = 0, y'' = 0, y''' = 0, A=1, f'=0, z' = 0$$

4. Result and Discussion

This section investigates the impact of various dimensionless numbers, including Weissenberg number (We), Magnetic number (M), Prandtl number (Pr), Eckert number (Ec), Velocity ratio parameter (A), Brownian motion parameter (Nb), Radiation parameter (Rd), Thermophoresis parameter (Nt), and Schmidt number (Sc), on velocity, temperature, and concentration profiles. The analysis aims to discern how these parameters influence the fluid flow, heat transfer, and mass transfer characteristics in the system under consideration. Figure 2 to Figure 13 analyse the variations of such parameters on the quantities. Table 2 additionally show the effect of relevant factors on the rate of mass transfer $Sh_x/\sqrt{Re_x}$, the rate of heat transfer $Nu_x/\sqrt{Re_x}$ and skin friction $\sqrt{Re_x}C_f$.

Figure 2 illustrates the impact of Prandtl number (Pr) on temperature (θ). Pr is the ratio of momentum diffusivity to thermal diffusivity. Rise in Prandtl number leads to the reduction in thermal diffusivity and the increase in momentum diffusivity due to this the thermal boundary layer thickness decreases and also temperature reduces more significantly.

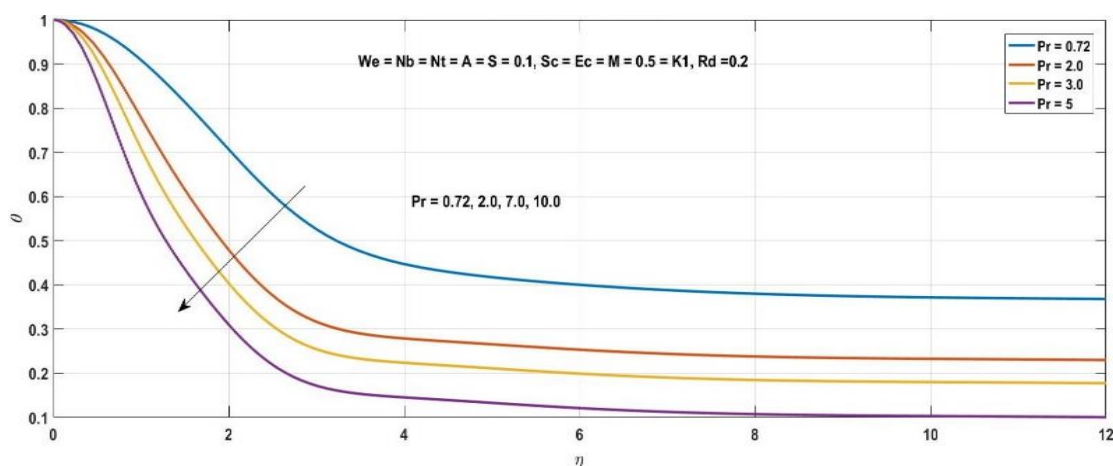


Fig. 2. Effects of Pr on temperature profile

Figure 3 explains the effects of Weissenberg number We on the velocity. Here We and velocity defined as f' and η . The Weissenberg number (We) is a dimensionless parameter employed in the analysis of viscoelastic flows, indicating the ratio of elastic to viscous effects in a material under deformation. We can observe that velocity and momentum boundary layer thickness decrease near the wall with increase in the value We there is rise in viscous force over the elasticity of the fluid. here, greater the viscous forces, smaller will be the velocity in the boundary layer region. But they disappear away from the wall.

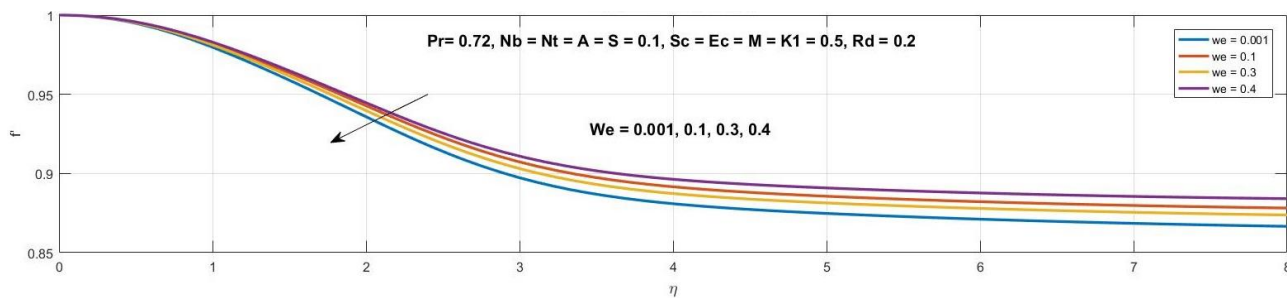


Fig. 3. Effects of We on velocity profile

In Figure 4, as temperature rises, the thermophoresis parameter (Nt) increases, indicating a higher thermophoretic force. Thermophoresis involves small particles exerting forces to move others away from a hotter surface towards a colder one. A higher Nt value corresponds to an increased thermophoretic force, and they push particles in the boundary layer from higher to lower temperature regions. Due to this there is increases in nanofluid temperature and nanoparticle concentration.

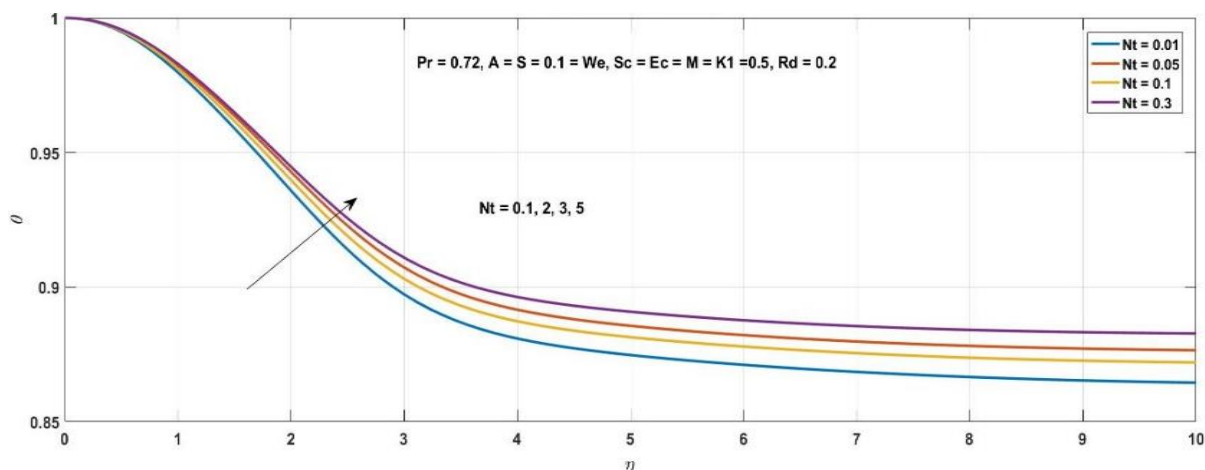


Fig. 4. Effects of Nt on temperature profile

In Figure 5, the impact of the velocity ratio parameter (A) on fluid velocity is illustrated. As A increases, both nanofluid velocity and momentum boundary layer thickness rise. This trend occurs when the free stream velocity is lower than that of the stretching sheet ($A < 1$).

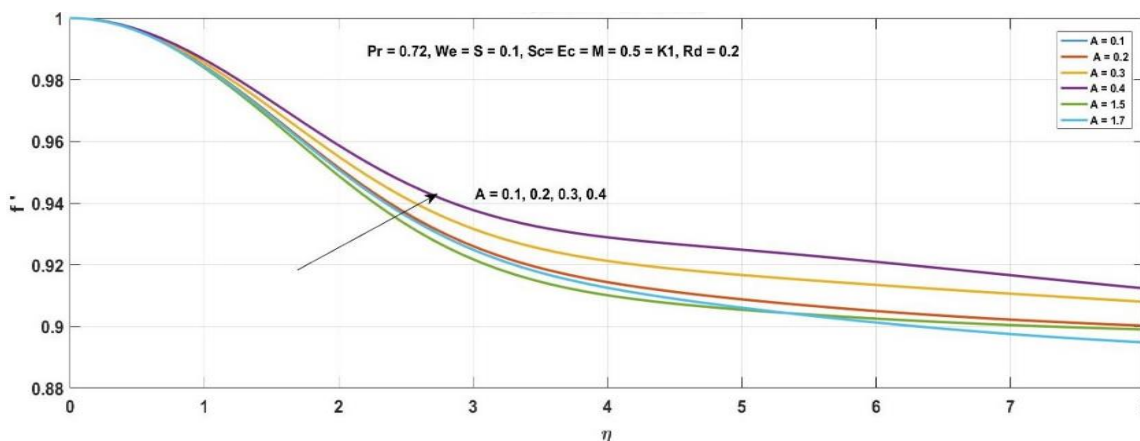


Fig. 5. Effects of A on velocity profile

In Figure 6, the relationship between Schmidt number (Sc) and nanoparticle volume fraction profiles is depicted. As Sc (momentum diffusivity to mass diffusivity ratio) increases, nanoparticle volume fraction decreases, indicating a correlation between Sc values and declining nanoparticle concentrations.

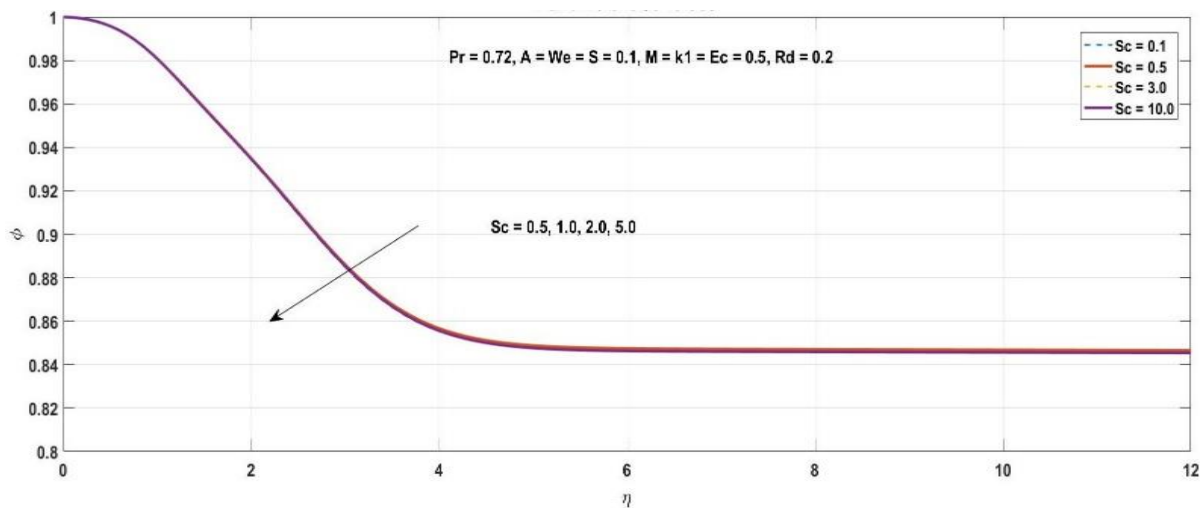


Fig. 6. Effects of Sc on concentration profile

Figure 7 illustrates how the temperature profile is influenced by the Eckert number (Ec), where the rise in Ec , caused by reduced nanoparticle volume fraction, leads to heightened temperature due to frictional heating.

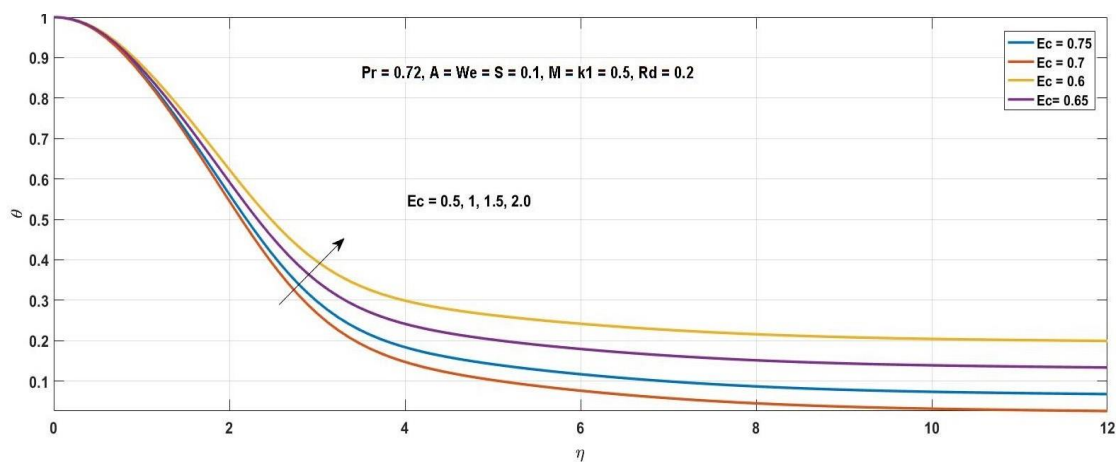


Fig. 7. Effects of Ec on temperature profile

Figure 8 similarly depicts the concentration profile affected by Ec . Additionally, Figure 9 highlights the impact of the radiation parameter (Rc) on temperature, showing that higher thermal radiation results in increased heat, leading to the expansion of the thermal boundary layer and elevated temperature profiles.

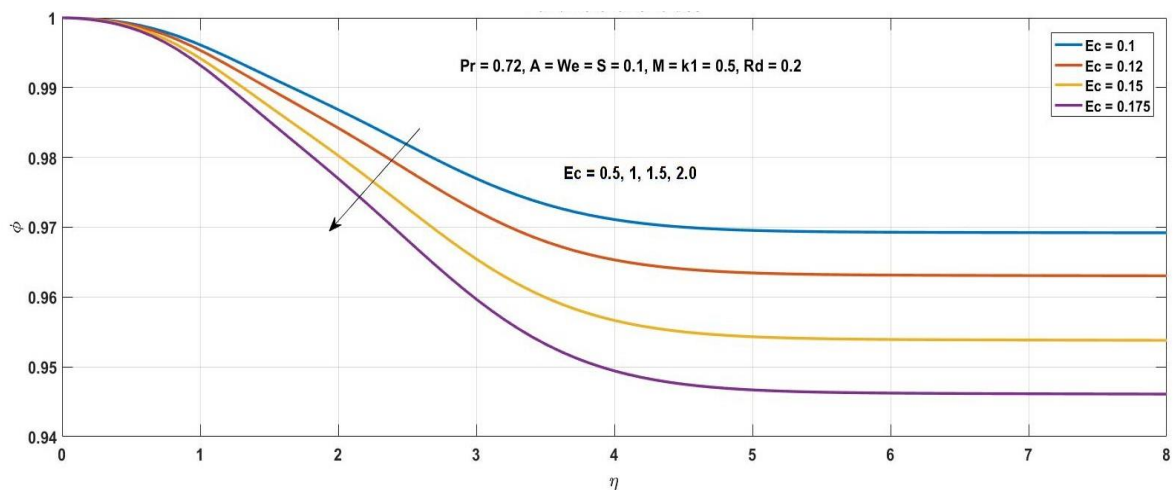


Fig. 8. Effects of Ec on concentration profile

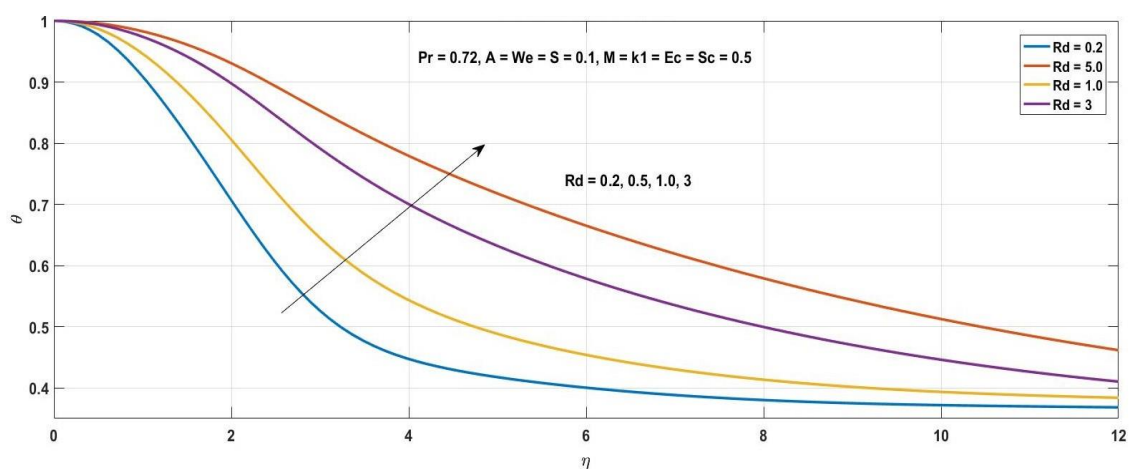


Fig. 9. Effects of Rd on temperature profile

Figure 10 and Figure 11 depict the impact of magnetic parameter (M) on velocity and temperature profiles. Increasing M results in a significant reduction in transport rate, indicating that the transverse magnetic field hinders transport phenomena due to heightened Lorentz force variation. This increased resistance causes velocity to diminish, particularly in the ambient region. Conversely, the temperature profile rises as M decreases.

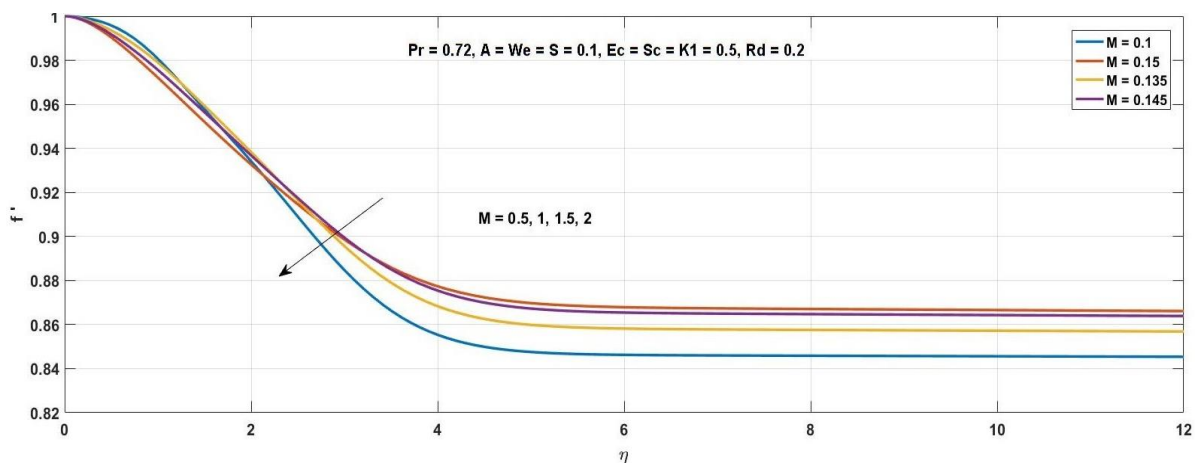


Fig. 10. Effects of M on velocity profile

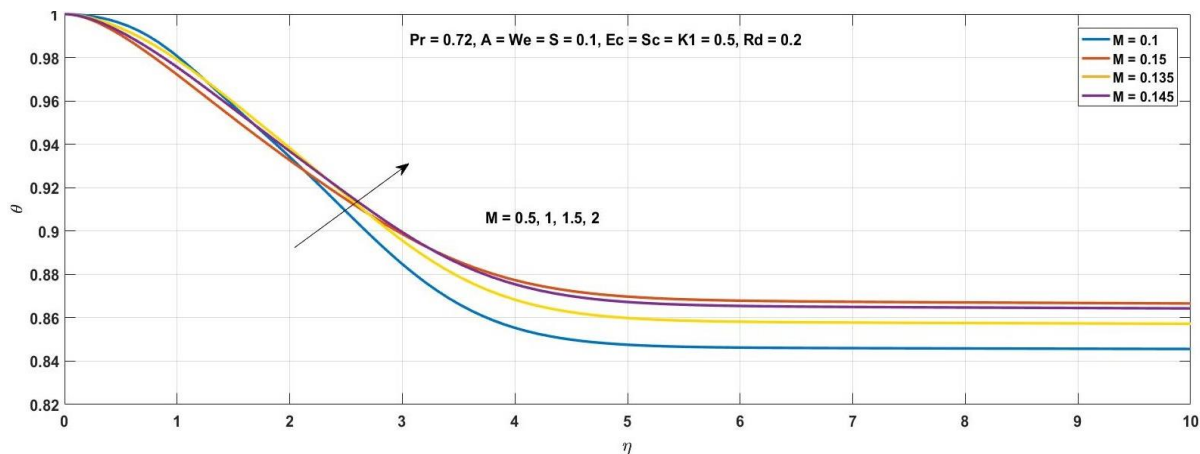


Fig. 11. Effects of M on temperature profile

Figure 12 and Figure 13 show the impact of wall mass transfer parameter (S) on temperature and velocity profiles. Increasing mass suction ($S > 0$) reduces boundary layer thickness, pulling fluid closer to the sheet and weakening both velocity and thermal profiles. Conversely, mass injection ($S < 0$) enhances profiles, broadening the boundary layers as fluid is pushed away from the sheet.

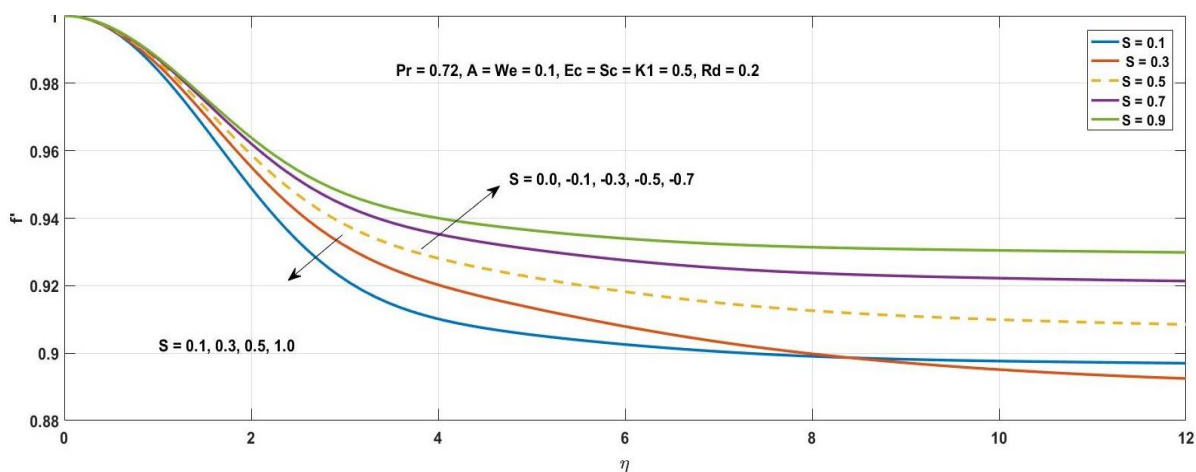


Fig. 12. Effects of S on Velocity profile

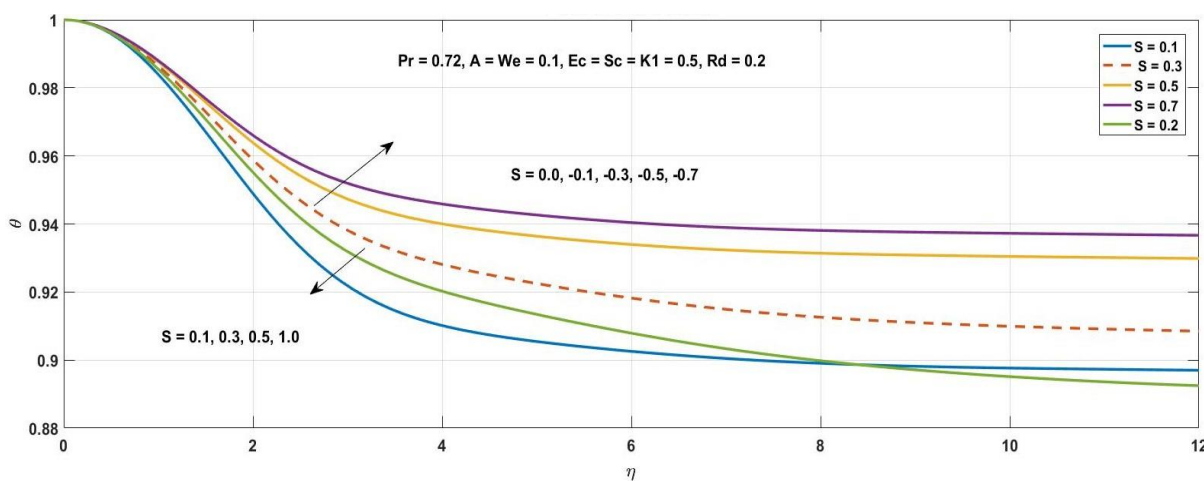


Fig. 13. Effects of S on temperature profile

Figure 14 and Figure 15 describe that decrease in concentration and thinner boundary layers were achieved through enhancements in the activation energy (E) and temperature difference (δ). Shows that concentration profile is not high through the increasing values of activation energy parameter E . It is watched that there is no sign to promote the concentration for the modified Arrhenius function, consequently, the general chemical reaction is improved.

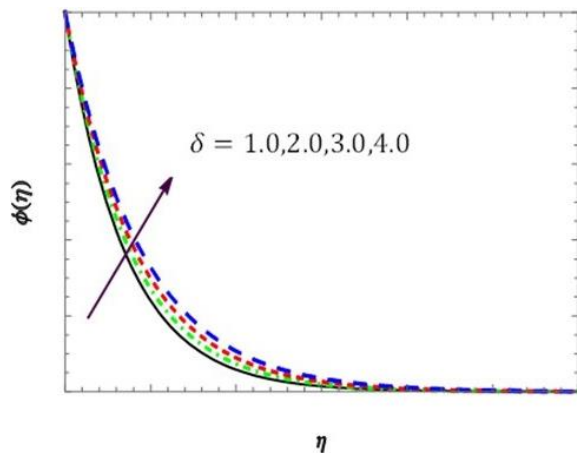


Fig. 14. Effects of δ on $\phi(\eta)$ with the values of ($Pr=1.0$; $E=1.0$; $Ec=Sc=0.1$)

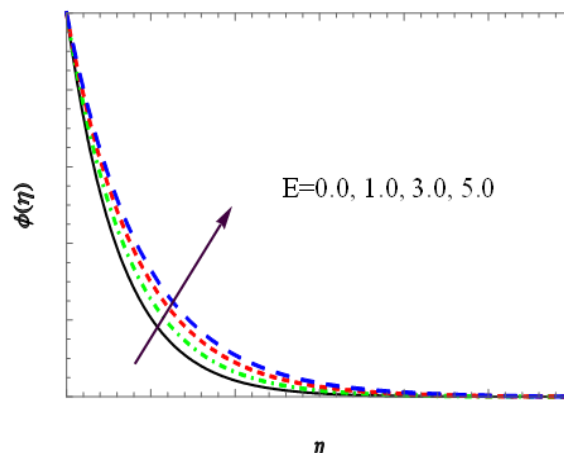


Fig. 15. Effects of E on $\phi(\eta)$ with the values of ($Pr=1.0$; $Ec=Sc=0.1$; $\delta=1.0$)

To confirm the precision of the numerical values, comparisons of were made with published works by Khan and Pop [11], Nadeem and Hussain [21] and Krishnamurthy *et al.*, [22] in the absence of Weissenberg and Eckert numbers, mass suction/injection, thermal radiation, magnetic field and chemical reaction parameters. The results are in nice agreement as shown in Table 1. Validation of the method enables us to investigate the effects of the physical parameters on the flow, temperature and concentration profiles. Moreover, the influences of these parameters on the skin friction coefficient and both heat and mass transfer rates are investigated.

Table 1

Comparison of the values of heat transfer rate $-\theta'(0)$ for different Prandtl numbers Pr values when $M = We = Ec = Rd = K_1 = A = S = Nt = 0$ and $Nb \rightarrow 0$

Pr	$-\theta'(0)$			
	Khan and Pop [11]	Nadeem and Hussain [21]	Krishnamurthy <i>et al.</i> , [22]	Present Study
0.07	0.0663	0.066	0.06624	0.066284
0.20	0.1691	0.169	0.16912	0.169123
0.70	0.4539	0.454	0.45432	0.454112
2.0	0.9113	0.911	0.91225	0.911212

The fluctuation of skin friction coefficient $\sqrt{Re_x} C_f$, reduced Nusselt number $Nu_x/\sqrt{Re_x}$ and reduced Sherwood number $Sh_x/\sqrt{Re_x}$ for different parameters are shown in Table 2. As shown in Table 2, the skin friction coefficient amplifies with higher Weissenberg number and suction parameter but declines with the velocity ratio parameter. The reduced Nusselt number rises with Weissenberg number, suction parameter, Reynolds number, and suction parameter, while declines with Prandtl number and velocity ratio parameter. Neither Schmidt number nor thermal conductivity has a significant impact. The reduced Sherwood number lessens with Weissenberg number and suction parameter, but increases with Nb , Sc , Ec , M , and K . The impact of Reynolds number on heat transfer is not significant.

Table 2
 Numerical values of Skin friction, Nusselt number and Sherwood number

Pr	We	Nb	A	Sc	Rd	K_1	S	$-\sqrt{Re_x} C_f$	$Nu_x/\sqrt{Re_x}$	$Sh_x/\sqrt{Re_x}$
0.72	0.1	0.1	0.1	0.5	0.2	0.5	0.1	1.179426	0.265749	0.660995
7.00								1.179426	0.241765	0.641471
10.0								1.179436	0.066478	0.627839
	0.3							1.322059	0.285744	0.825471
	0.4							1.457171	0.299747	0.845829
		2.0						1.179418	-0.032334	0.651589
		3.0						1.179418	-0.092135	0.648991
		5.0						1.179418	-0.129557	1.0088401
			0.2					1.096821	0.304446	1.511622
			0.3					1.000221	0.328471	2.563821
			0.4					0.891434	0.340554	0.833291
				1.0				1.179418	0.262793	1.005729
				2.0				1.179417	0.260923	1.178333
				5.0				1.179416	0.260055	0.664892
					0.5			1.179415	0.309402	0.668382
					1.0			1.179426	0.368894	0.670658
					3.0			1.179426	0.531814	0.724723
						1.0		1.179426	0.263938	0.780301
						2.0		1.179426	0.262297	0.830017
						3.0		1.179426	0.261517	0.877039
							0.3	1.276155	0.347433	1.175822
							0.5	1.379645	0.434125	1.400581
							1.0	1.666221	0.668041	0.660997

5. Conclusions

After reviewing the issue of MHD in two-dimensional flow across a permeable stretched sheet with a Williamson nanofluid when viscous dissipation, heat radiation, and Arrhenius activation energy are present. Using suitable similarity transformation equations, the nonlinear linked ODEs were created using nonlinear differential equations pertaining to the boundary conditions. The RK-method was used to answer the issues numerically, and it was combined with the shooting approach. Among the many significant findings, a few are enumerated here

- i. The velocity profile rises as the velocity ratio parameter increases, but it falls when magnetic parameter, Weissenberg number and mass suction parameter increases.
- ii. The temperature profile is significantly decreased by the Prandtl number and mass suction parameter, whereas it is greatly increased by Eckert number, magnetic, thermal radiation and thermophoresis factors.
- iii. It is noted that when both the Schmidt and Eckert numbers increase, the profile of volume fraction of the nanoparticles diminishes.
- iv. Research shows that heat transfer rate reduces as the values of the parameters Pr , Nb , Sc , Rd and k ascends, it is enhanced by the values of We , A and S .
- v. It is seen that the mass transfer rate rises with rising parameters Nb , Sc , Ec , Rd , M and k , but falls with increasing values of We and A .
- vi. A decrease in concentration and thinner boundary layers were achieved through enhancements in the activation energy (E) and temperature difference (δ).
- vii. The use of Arrhenius activation energy in Williamson nanofluid research facilitates a deeper understanding of temperature dependent properties and behaviour, which is essential for designing and optimising nanofluid based thermal management system.

References

- [1] Yang, Jiawang, Xian Yang, Jin Wang, Hon Huin Chin, and Bengt Sundén. "Review on thermal performance of nanofluids with and without magnetic fields in heat exchange devices." *Frontiers in Energy Research* 10 (2022): 822776. <https://doi.org/10.3389/fenrg.2022.822776>
- [2] Ali, Abu Raihan Ibna, and Bodius Salam. "A review on nanofluid: preparation, stability, thermophysical properties, heat transfer characteristics and application." *SN Applied Sciences* 2, no. 10 (2020): 1636. <https://doi.org/10.1007/s42452-020-03427-1>
- [3] Saxena, Divya. "Study of viscous dissipation and convection of heat transfer over a flat plate with variable temperature using homotopy perturbation technique." In *Proceedings of International Conference on Advancements in Computing & Management (ICACM)*. 2019.
- [4] Li, Junhao, Xilong Zhang, Bin Xu, and Mingyu Yuan. "Nanofluid research and applications: A review." *International Communications in Heat and Mass Transfer* 127 (2021): 105543. <https://doi.org/10.1016/j.icheatmasstransfer.2021.105543>
- [5] Adnan, Umar Khan, Naveed Ahmed, Syed Tauseef Mohyud-Din, M. D. Alsulami, and Ilyas Khan. "A novel analysis of heat transfer in the nanofluid composed by nanodiamond and silver nanomaterials: numerical investigation." *Scientific Reports* 12, no. 1 (2022): 1284. <https://doi.org/10.1038/s41598-021-04658-x>
- [6] Ajibade, Abiodun O., Ayuba M. Umar, and Tafida M. Kabir. "An analytical study on effects of viscous dissipation and suction/injection on a steady mhd natural convection couette flow of heat generating/absorbing fluid." *Advances in Mechanical Engineering* 13, no. 5 (2021): 16878140211015862. <https://doi.org/10.1177/16878140211015862>
- [7] Rehman, Ali, Zabidin Salleh, Taza Gul, and Zafar Zaheer. "The impact of viscous dissipation on the thin film unsteady flow of GO-EG/GO-W nanofluids." *Mathematics* 7, no. 7 (2019): 653. <https://doi.org/10.3390/math7070653>
- [8] Ajayi, T. M., A. J. Omowaye, and Isaac Lare Animasaun. "Viscous dissipation effects on the motion of Casson fluid over an upper horizontal thermally stratified melting surface of a paraboloid of revolution: boundary layer analysis." *Journal of Applied Mathematics* 2017 (2017). <https://doi.org/10.1155/2017/1697135>
- [9] Hassan, Ali, Azad Hussain, Mubashar Arshad, Soumaya Gouadria, Jan Awrejcewicz, Ahmed M. Galal, Fahad M. Alharbi, and S. Eswaramoorthi. "Insight into the significance of viscous dissipation and heat generation/absorption in magneto-hydrodynamic radiative casson fluid flow with first-order chemical reaction." *Frontiers in Physics* 10 (2022): 920372. <https://doi.org/10.3389/fphy.2022.920372>
- [10] Eswaramoorthi, S., Nazek Alessa, M. Sangeethavaanee, Safak Kayikci, and Ngawang Namgyel. "Mixed convection and thermally radiative flow of MHD Williamson nanofluid with Arrhenius activation energy and Cattaneo-Christov heat-mass flux." *Journal of Mathematics* 2021 (2021): 1-16. <https://doi.org/10.1155/2021/2490524>
- [11] Khan, W. A., and I. Pop. "Boundary-layer flow of a nanofluid past a stretching sheet." *International Journal of Heat and Mass Transfer* 53, no. 11-12 (2010): 2477-2483. <https://doi.org/10.1016/j.ijheatmasstransfer.2010.01.032>
- [12] Pearson, J. R. A., and P. M. J. Tardy. "Models for flow of non-Newtonian and complex fluids through porous media." *Journal of Non-Newtonian Fluid Mechanics* 102, no. 2 (2002): 447-473. [https://doi.org/10.1016/S0377-0257\(01\)00191-4](https://doi.org/10.1016/S0377-0257(01)00191-4)
- [13] Kalaivanan, R., N. Vishnu Ganesh, and Qasem M. Al-Mdallal. "An investigation on Arrhenius activation energy of second grade nanofluid flow with active and passive control of nanomaterials." *Case Studies in Thermal Engineering* 22 (2020): 100774. <https://doi.org/10.1016/j.csite.2020.100774>
- [14] Mozafarie, Seyed Shahab, and Kourosh Javaherdeh. "Numerical design and heat transfer analysis of a non-Newtonian fluid flow for annulus with helical fins." *Engineering Science and Technology, an International Journal* 22, no. 4 (2019): 1107-1115. <https://doi.org/10.1016/j.jestch.2019.03.001>
- [15] Sheikholeslami, Mohsen, M. M. Rashidi, and D. D. Ganji. "Effect of non-uniform magnetic field on forced convection heat transfer of Fe₃O₄-water nanofluid." *Computer Methods in Applied Mechanics and Engineering* 294 (2015): 299-312. <https://doi.org/10.1016/j.cma.2015.06.010>
- [16] Li, Yanjiao, Simon Tung, Eric Schneider, and Shengqi Xi. "A review on development of nanofluid preparation and characterization." *Powder Technology* 196, no. 2 (2009): 89-101. <https://doi.org/10.1016/j.powtec.2009.07.025>
- [17] Rasheed, Haroon U. R., Saeed Islam, Zeeshan Khan, Sayer O. Alharbi, Hammad Alotaibi, and Ilyas Khan. "Impact of nanofluid flow over an elongated moving surface with a uniform hydromagnetic field and nonlinear heat reservoir." *Complexity* 2021 (2021): 1-9. <https://doi.org/10.1155/2021/9951162>
- [18] Giresha, B. J., and N. G. Rudraswamy. "Chemical reaction on MHD flow and heat transfer of a nanofluid near the stagnation point over a permeable stretching surface with non-uniform heat source/sink." *International Journal of Engineering, Science and Technology* 6, no. 5 (2014): 13-25. <https://doi.org/10.4314/ijest.v6i5.2>
- [19] Sheri, Siva Reddy, and Thirupathi Thumma. "Numerical study of heat transfer enhancement in MHD free convection flow over vertical plate utilizing nanofluids." *Ain Shams Engineering Journal* 9, no. 4 (2018): 1169-1180. <https://doi.org/10.1016/j.asej.2016.06.015>

- [20] Choi, S. U. S., and Jeffrey A. Eastman. *Enhancing thermal conductivity of fluids with nanoparticles*. No. ANL/MSD/CP-84938; CONF-951135-29. Argonne National Lab.(ANL), Argonne, IL (United States), 1995.
- [21] Nadeem, S., and S. T. Hussain. "Flow and heat transfer analysis of Williamson nanofluid." *Applied Nanoscience* 4 (2014): 1005-1012. <https://doi.org/10.1007/s13204-013-0282-1>
- [22] Krishnamurthy, M. R., B. C. Prasannakumara, B. J. Gireesha, and Rama Subba Reddy Gorla. "Effect of chemical reaction on MHD boundary layer flow and melting heat transfer of Williamson nanofluid in porous medium." *Engineering Science and Technology, an International Journal* 19, no. 1 (2016): 53-61. <https://doi.org/10.1016/j.jestch.2015.06.010>
- [23] Gorfie, Eshetu Haile, Gurju Awgichew Zergaw, and Hunegnaw Dessie Assres. "Thermally radiant williamson nanofluid flow over a permeable stretching sheet with viscous dissipation and joule heating effects." *Journal of Nanofluids* 11, no. 3 (2022): 401-409. <https://doi.org/10.1166/jon.2022.1852>
- [24] Lavanya, Bommanna. "Radiation and chemical reaction effects on MHD convective flow over a porous plate through a porous medium with heat generation." *Journal of Advanced Research in Fluid Mechanics and Thermal Sciences* 68, no. 1 (2020): 11-21. <https://doi.org/10.37934/arfmts.68.1.1121>
- [25] Kumar, R. V. M. S. S. Kiran, G. Vinod Kumar, C. S. K. Raju, S. A. Shehzad, and S. V. K. Varma. "Analysis of Arrhenius activation energy in magnetohydrodynamic Carreau fluid flow through improved theory of heat diffusion and binary chemical reaction." *Journal of Physics Communications* 2, no. 3 (2018): 035004. <https://doi.org/10.1088/2399-6528/aaafff>
- [26] Vijaya, N., S. M. Arifuzzaman, N. Raghavendra Sai, and Manikya Rao. "Analysis of Arrhenius activation energy in electrically conducting casson fluid flow induced due to permeable elongated sheet with chemical reaction and viscous dissipation." *Frontiers in Heat and Mass Transfer (FHMT)* 15, no. 1 (2020). <https://doi.org/10.5098/hmt.15.26>
- [27] Nagasasikala, Madduleti, and Bommanna Lavanya. "Heat and mass transfer of a MHD flow of a nanofluid through a porous medium in an annular, circular region with outer cylinder maintained at constant heat flux." *CFD Letters* 11, no. 9 (2019): 32-58.
- [28] Akaje, Wasiu, and B. I. Olajuwon. "Impacts of Nonlinear thermal radiation on a stagnation point of an aligned MHD Casson nanofluid flow with Thompson and Troian slip boundary condition." *Journal of Advanced Research in Experimental Fluid Mechanics and Heat Transfer* 6, no. 1 (2021): 1-15.
- [29] Al-Shammari, Hammad, Zia Ullah, Fethi Albouchi, Asifa Ilyas, Musaad S. Aldhabani, Haifaa F. Alrihieli, Mohamed Boujelbene, and Ahmed M. Hassan. "Primitive and gravity modulation of periodical heat transfer along magnetic-driven porous cone with thermal conductivity and surface heat flux." *Case Studies in Thermal Engineering* 53 (2024): 103866. <https://doi.org/10.1016/j.csite.2023.103866>
- [30] Ullah, Zia, Musaad S. Aldhabani, and Muhammad Adnan Qaiser. "Oscillatory and Periodical Behavior of Heat Transfer and Magnetic Flux along Magnetic-Driven Cylinder with Viscous Dissipation and Joule Heating Effects." *Mathematics* 11, no. 18 (2023): 3917. <https://doi.org/10.3390/math11183917>